

# Beyond the bubble catastrophe of Type Ia supernovae: Pulsating Reverse Detonation models

Eduardo Bravo<sup>1,2</sup>, Domingo García-Senz<sup>1,2</sup>

## ABSTRACT

We describe a mechanism by which a failed deflagration of a Chandrasekhar-mass carbon-oxygen white dwarf can turn into a successful thermonuclear supernova explosion, without invoking an *ad hoc* high-density deflagration-detonation transition. Following a pulsating phase, an accretion shock develops above a core of  $\sim 1 M_{\odot}$  composed of carbon and oxygen, inducing a converging detonation. A three-dimensional simulation of the explosion produced a kinetic energy of  $1.05 \times 10^{51}$  ergs and  $0.70 M_{\odot}$  of  $^{56}\text{Ni}$ , ejecting scarcely  $0.01 M_{\odot}$  of C-O moving at low velocities. The mechanism works under quite general conditions and is flexible enough to account for the diversity of normal Type Ia supernovae. In given conditions the detonation might not occur, which would reflect in peculiar signatures in the gamma and UV-wavelengths.

*Subject headings:* Supernovae: general – hydrodynamics – nuclear reactions, nucleosynthesis, abundances – ultraviolet: stars

## 1. Introduction

In order to measure cosmic distances with the precision required to determine the equation of state of the dark energy component of our Universe, it is necessary to understand the physics of Type Ia supernovae (SNIa). From the theoretical point of view, the accepted model of SNIa consists of a Chandrasekhar-mass white dwarf (WD) that accretes matter from a close binary companion. This scenario accounts for the SNIa sample homogeneity,

---

<sup>1</sup>Dept. Física i Enginyeria Nuclear, Univ. Politècnica de Catalunya, Diagonal 647, 08028 Barcelona, Spain; eduardo.bravo@upc.edu domingo.garcia@upc.edu

<sup>2</sup>Institut d'Estudis Espacials de Catalunya, Barcelona, Spain

the lack of hydrogen in their spectra, and its detection in elliptical galaxies. There are two main ingredients of the standard model that are still poorly known: the precise configuration and evolution of the binary system prior to thermal runaway of the WD, and the explosion mechanism. In spite of 40 years of theoretical efforts dedicated to understand the mechanism behind SNIa, realistic simulations are still unable to provide a satisfactory description of the thermonuclear explosion. Nowadays, there is consensus that the initial phases of the explosion involve a subsonic thermonuclear flame (deflagration), whose propagation competes with the expansion of the WD. After a while the corrugation of the flame front induced by hydrodynamic instabilities leads to an acceleration of the effective combustion. The nature of the events that follow is currently under debate between advocates of a transition to a supersonic detonation front and those defending that the flame remains subsonic. Recent three-dimensional (3D) models calculated by different groups have shown that both explosion mechanisms display positive as well as serious weak points. Pure deflagrations always give final kinetic energies that fall short of  $10^{51}$  ergs and leave too much unburnt carbon and oxygen (C-O) close to the center (Gamezo et al. 2003; Hillebrandt and Niemeyer 2000; Reinecke, Hillebrandt, and Niemeyer 2002). Both results are at odds with observational constraints. Leaving aside pure deflagrations, Gamezo et al. (2003) proposed that it would be necessary to assume that the turbulent flame triggers a detonation. On the other hand, the deflagration-detonation transition (DDT) had to be postulated *ad hoc* (Arnett and Livne 1994; Höflich, Khokhlov, and Wheeler 1995), because current numerical experiments disfavour such a transition in exploding WDs (Niemeyer 1999).

In Bravo and García-Senz (2005) it was sketched a mechanism through which a delayed detonation might naturally arise: the Pulsating Reverse Detonation (PRD) model. In the PRD paradigm the explosion proceeds in three steps: 1) an initial pre-conditioning phase whose result is the inversion of the chemical structure of the progenitor WD, 2) the formation of an accretion shock that confines the fuel and, 3) the launch of an inward moving detonation. In this Letter we present the results of 3D simulations of the PRD model. In the next section we describe our simulations and analyse the properties of the accretion shock, while in the final section we speculate about the implications of this new paradigm of SNIa. A more detailed report with additional calculations of the PRD model will be published elsewhere (Bravo & García-Senz, in preparation).

## 2. The Pulsating Reverse Detonation model

Our initial model consists of a  $1.38 M_{\odot}$  C-O WD. The hydrodynamic evolution started with the ignition of 6 sparks [model B06U in Garcia-Senz and Bravo (2005)] incinerating

$M_{\text{def}} = 0.18 M_{\odot}$  in one second, while releasing  $2.5 \times 10^{50}$  ergs of nuclear energy which led to the pulsation of the star.

The details of the first phase, that spans the first two seconds after thermal runaway, have been known for some time (Plewa, Calder, and Lamb 2004; Livne, Asida, and Höflich 2005). Even though the precise configuration at thermal runaway is difficult to determine, current works suggest a multipoint ignition in which the first sparks are located slightly off-center (García-Senz and Woosley 1995; Woosley, Wunsch, and Kuhlen 2004). If the number of sparks is too small the nuclear energy released is not enough to unbind the star and the explosion fails. This is known as the "single-bubble catastrophe" (Livne, Asida, and Höflich 2005). These bubbles float to the surface before the combustion wave can propagate substantially (Plewa, Calder, and Lamb 2004; Garcia-Senz and Bravo 2005) and the star remains energetically bound. This behaviour produces a composition inversion, i.e. the fuel, composed of cold C-O, fills the internal volume while the ashes of the initial combustion, mostly hot iron and nickel, are scattered around (Fig. 1). In the 3D calculations the energy resides for the most part in the outer  $0.15 M_{\odot}$ . Hence, the expanding motion of the external material is decoupled from the rest of the structure, and a pulsation starts.

The second phase of the explosion begins when the deflagration quenches due to expansion and ends when an accretion shock is formed by the impact of the infalling material. At the end of this phase, the inner  $1.0 M_{\odot}$  C-O rich core adopts an equilibrium configuration inertially confined by an accretion shock (Fig. 1). Before describing the events that ensue to the formation of the accretion shock, we will perform an analysis of its properties, based on the structure of the shock resulting from our simulation of the first pulsation of the WD. We show that a detonation is expected to start a few thousand kms below the accretion shock and that, once formed, it cannot be quenched due to a rapid expansion of the core, which remains confined due to the large impact pressure of the accreting matter. This analysis is intended to provide the physical basis for the formation of the detonation in order to support the results of our hydrodynamical calculations, which might be affected by numerical resolution.

The structure of the WD at  $t = 7.18$  s can be seen in Fig. 1. Below  $\sim 15,000$  km matter is flowing in towards the hydrostatic core. The accretion shock starts at  $r_{\text{sh}} \sim 5,000$  km (lagrangian mass  $\sim 1.17 M_{\odot}$ ), where the inwards velocity of the infalling matter is  $v_r \sim 5,000$  km·s<sup>-1</sup>. The density just above the accretion shock is  $\rho_0 = 8.3 \times 10^4$  g·cm<sup>-3</sup>, while that of shocked matter rises to  $\rho_{\text{sh}} = 4\rho_0 = 3.3 \times 10^5$  g·cm<sup>-3</sup>. Once formed, the accretion shock remains confined close to the hydrostatic core due to the large impact pressure of the infalling matter compared to the gas pressure behind the shock:  $\rho v^2/p = \gamma M^2 \sim 12$ , where  $\rho v^2$  is the impact pressure,  $p$  is the gas pressure,  $\gamma = 5/3$  is the adiabatic coefficient, and  $M$  is

the Mach number. We can reformulate this point in a more quantitative way as follows. The rate of mechanical energy deposition at the accretion shock is given by  $\dot{\epsilon}_{\text{mec}} = 2\pi r^2 \rho_0 v^3$ , which can be compared to the rate of nuclear energy released in a combustion front propagating at velocity  $c$ ,  $\dot{\epsilon}_{\text{nuc}} = 4\pi r^2 \rho_{\text{sh}} c q$ , where  $q \sim 5.8 \times 10^{17} \text{ erg}\cdot\text{g}^{-1}$  is the difference in nuclear binding energy between matter composed of C-O and  $^{28}\text{Si}$ . Equating both energy rates one obtains  $c = 270 \text{ km}\cdot\text{s}^{-1}$ . This is roughly the flame velocity that would be required to revert the bulk inward motion of the accreting matter. It turns out that this velocity is  $\sim 0.1 v_{\text{sound}}$ , that is much larger than the maximum velocity of a stable deflagration at  $\rho_{\text{sh}}$  (Khokhlov 1988),  $v_{\text{sound}}$  being the local sound velocity. Furthermore, due to the converging nature of the combustion wave the fuel has nowhere to expand, ensuring that the flame will not be quenched.

There is an additional condition for detonation initiation: the nuclear time scale must be lower than the hydrodynamical timescale. The temperature attained at the accretion shock can be estimated from the Rankine-Hugoniot conditions for a strong shock and the ideal gas equation of state, giving  $T_{\text{sh}} = (3/16) (\mu/k_{\text{B}} N_{\text{A}}) v^2$ , where  $\mu$  is the mean molar mass,  $N_{\text{A}}$  is Avogadro's number, and  $k_{\text{B}}$  is the Boltzmann constant. In matter composed of completely ionized C-O,  $\mu = 1.75 \text{ g}\cdot\text{mol}^{-1}$ , which gives  $T_{\text{sh}} = 10^9 \text{ K}$ . At the density of the shock, this temperature is not high enough to burn in less than a hydrodynamical time,  $\tau_{\text{hyd}} = 446/\sqrt{\rho_{\text{sh}}} = 0.78 \text{ s}$ , thus the shocked matter must be compressed further along its path towards the surface of the hydrostatic core before detonating. Due to the high accretion rate, the shocked gas remains optically thick and photons are trapped in the infalling matter, implying that radiative cooling is inefficient and the flow is radiation dominated, i.e. the adiabatic coefficient goes down to  $\gamma = 4/3$ . Assuming an adiabatic evolution of this radiation-dominated shocked matter,  $T \propto \rho^{1/3}$ , one can compare the local values of the nuclear timescale,  $\tau_{\text{nuc}}$ , and  $\tau_{\text{hyd}}$  in order to find the radius at which explosive ignition is reliable. With the additional approximations of steady state and spherical symmetry the structure of the shocked flow between the accretion shock and the core can be obtained by solving the following set of equations:  $e = v^2/2 + p/[\rho(\gamma - 1)] - GM/r = \text{constant}$  (conservation of energy),  $\rho v r^2 = \text{constant}$  (conservation of mass), and  $p \propto \rho^{4/3}$  (adiabatic evolution), starting from the physical state behind the shock,  $\rho_{\text{sh}}$ ,  $T_{\text{sh}}$ , and  $v_{\text{sh}} = v/4 = 1,250 \text{ km}\cdot\text{s}^{-1}$ . We have found that  $\tau_{\text{nuc}} < \tau_{\text{hyd}}$  at  $r_{\text{det}} = 3,400 \text{ km}$  and  $\rho_{\text{det}} = 1.3 \times 10^6 \text{ g}\cdot\text{cm}^{-3}$ , i.e. a detonation is able to form  $0.12 M_{\odot}$  inside the accretion shock. It turns out that the ignition of a detonation critically depends on the amount of mass burnt during the deflagration phase: the larger  $M_{\text{def}}$  the more difficult is the formation of a detonation. In another model that burned  $M_{\text{def}} = 0.29 M_{\odot}$  subsonically, the temperature and density behind the shock rised only to  $4.5 \times 10^8 \text{ K}$  and  $1.4 \times 10^5 \text{ g}\cdot\text{cm}^{-3}$ . Eventually, one can expect that increasing slightly the value of  $M_{\text{def}}$  the physical conditions behind the shock would not allow the formation of

a stable burning front and the explosion would finally fail. We expect such a failure for a narrow range of  $M_{\text{def}} \sim 0.29 - 0.35 M_{\odot}$ , in which case the event would not resemble a SNIa.

The third phase of the explosion starts when the converging reverse detonation wave is launched. This phase has been computed with our 3D hydrodynamical code, the same as in García-Senz, Bravo and Woosley (1999) although with higher resolution (here, we used 250,000 particles). In our model the detonation starts naturally as a result of the compressional heating caused by the accretion shock and, once initiated, the detonation is self-sustained by the burning of fuel either to intermediate-mass or to Fe-group elements. During the first 0.3 s after detonation ignition the accretion shock remains stationary, close to the core (Fig.2). Afterwards, the overpressure generated by the nuclear energy released pushes outwards the accretion shock, that detaches from the core, and the detonated matter starts to expand with large velocities. The expansion weakens the detonation and finally the burning quenches. As a result, the detonation burns all the fuel except for a tiny region at the center. In the outer layers of the hydrostatic core the density is low enough to allow incomplete burning and leave a composition rich in intermediate mass elements (Fig.3) while in the inner regions the burning proceeds all the way up to  $^{56}\text{Ni}$  (the central density at the moment of formation of the detonation is  $10^8 \text{ g}\cdot\text{cm}^{-3}$ ). The simulation was ended when the elapsed time was 5176 s after initial thermal runaway.

How do the hydrodynamical simulations of the PRD model compare to observations of SNIa? Nowadays, a detailed comparison with existing data is not possible because multi-dimensional spectral and photometric codes are not fully developed. However, in general terms, our results match quite satisfactorily basic SNIa observational constraints. The mechanical structure of the ejecta retains a high degree of spherical symmetry and is chemically stratified, although there is some small-scale mixing and clumping of chemical elements. The final kinetic energy is  $1.05 \times 10^{51}$  ergs, and the total amount of  $^{56}\text{Ni}$  produced in the event is  $0.70 M_{\odot}$ , in good agreement with what is demanded by observations of typical SNIa (Branch and Khokhlov 1995). There remain only  $0.06 M_{\odot}$  of unburned C, most of it moving at high velocities. This carbon, as well as the remaining unburned O (Table1) would be hardly detectable around the epoch of maximum light (Baron, Lentz, and Hauschildt 2003). The total amount of C-O moving at low velocities is  $0.01 M_{\odot}$ , that is within the limits derived by Kozma et al. (2005) from late-time spectra. Intermediate mass elements moving at velocities  $> 8,000 \text{ km}\cdot\text{s}^{-1}$  are abundant at the photospheric radius at maximum light, as required by observations.

### 3. Discussion

In the beginning, the motivation of our calculation was to reproduce a 3D analogue of the Pulsating Delayed Detonation (PDD) model introduced by Ivanova, Imshennik, and Chechetkin (1974) and developed by Khokhlov (1991). In both the PDD and the PRD models there is an initial unsuccessful deflagration phase leading to a pulsation of the WD. However, in the PDD model the incinerated matter stays at the center, and there is neither composition inversion nor accretion shock. Thus, the mechanism of formation of a detonation and the final result is quite different in both kind of models.

The PRD paradigm is capable of producing a variety of outcomes, which could account for a part of the observed diversity of SNIa. This variety derives from differences in the mass of the hydrostatic core at the moment of formation of the accretion shock, and is allowed by the general validity of the mechanism of initiation of the detonation. We have performed a preliminary exploration of the sensitivity of the explosion properties to the mass of the hydrostatic core by means of 1D hydrodynamic calculations (Bravo & García-Senz, in preparation). For reasonable choices of the core mass, the final kinetic energies range from  $0.72 \times 10^{51}$  up to  $1.21 \times 10^{51}$  erg, and the  $^{56}\text{Ni}$  masses from 0.35 to 0.88  $M_{\odot}$ . This range would translate in differences of up to 1 mag, in fairly agreement with the observational range of absolute magnitudes of *normal* SNIa (from  $M_B = -18.62$  for SN1983G to  $M_B = -19.69$  for SN1997bp).

The origin of the variation of core masses could be due to a randomness of the number of sparks igniting initially at the centre of accreting WDs. A large number of sparks would imply a larger nuclear energy release during the deflagration phase, thus a smaller fuel-rich hydrostatic core after initial pulsation and a more loose structure at the moment of accretion shock formation, leading to lower values of the final kinetic energy and  $^{56}\text{Ni}$  mass. The initial number of sparks could also be related to the rotation of the WD (Kuhlen, Woosley, and Glatzmaier 2005), a lower number being favoured in slow rotators, opening an interesting connection between the pre-supernova evolution of the binary system and the explosion properties.

We have identified two possible observational tests of the PRD paradigm, both of them related to the eventual failure to develop a detonation (thus not giving a SNIa-like phenomenon) if the mass burned prior to pulsation lies in the range  $\sim 0.29 - 0.35 M_{\odot}$ . First, even in the absence of a detonation the outermost  $\sim 0.23 - 0.28 M_{\odot}$  (half of which  $^{56}\text{Ni}$ ) would have enough energy to escape from the WD. Due to the low column density, the radioactive photons emitted in the disintegration of  $^{56}\text{Ni}$  and  $^{56}\text{Co}$  would not be efficiently thermalized to optical wavelengths. We have estimated that during the first 30-40 days the gamma-ray spectrum would be similar to the one predicted for sub-Chandrasekhar models

(Milne et al. 2004), but after  $\sim 50$  days, when the ejected matter becomes optically thin, the continuum and 511 keV lines would turn much fainter, due to the smaller mass of  $^{56}\text{Ni}$  synthesized. Second, the small amount of mass ejected would not be enough to destroy the binary system. The stellar remnant left back by the failed supernova would be characterized for some time by a high luminosity in the UV, an exotic surface chemical composition (rich in C, O, Fe and Ni), an eccentric orbit, and a mass  $\sim 1.10 - 1.15 M_{\odot}$ . The detection of such objects and the measurement of its properties might provide important information about the final fate of WDs experiencing ignition in a few bubbles.

This work has been supported by DURSI of the Generalitat de Catalunya and Spanish DGICYT grants AYA2000-1785, AYA2001-2360 and AYA2002-04094. In loving memory of María del Llano and L. Alexandra.

## REFERENCES

- Arnett, W.D., & Livne, E. 1994, *ApJ*, 427, 330
- Baron, E., Lentz, E.J., & Hauschildt, P.H. 2003, *ApJ*, 588, L29
- Branch, D., & Khokhlov, A. 1995, *Phys. Rep.*, 256, 53
- Bravo, E., & García-Senz, D. 2005, in *Cosmic Explosions. On the 10th Anniversary of SN1993J (IAU Coll. 192)*, eds. J. Marcaide & K.W. Weiler (Berlin: Springer), 339-344 (astro-ph/0401230)
- Gamezo, V.N., Khokhlov, A.M., Oran, E.S., Ctchelkanova, A.Y., & Rosenberg, R.O. 2003, *Science*, 299, 77
- García-Senz, D., Bravo, E., 2005, *A&A*, 430, 585
- García-Senz D., Bravo, E., & Woosley, S.E. 1999, *A&A*, 349, 177
- García-Senz D., & Woosley, S.E. 1995, *ApJ*, 454, 895
- Hillebrandt, W., & Niemeyer, J. 2000, *ARA&A*, 38, 191
- Höfllich, P., Khokhlov, A., & Wheeler, J.C. 1995, *ApJ*, 444, 831
- Ivanova, L.N., Imshennik, V.S., & Chechetkin, V.M. 1974, *Ap&SS*, 31, 497
- Khokhlov, A. 1988, *Ap&SS*, 149, 91



Khokhlov, A. 1989, MNRAS, 239, 785

Khokhlov, A. 1991, A&A, 245, L25

Kozma, C., Fransson, C., Hillebrandt, W., Travaglio, C., Sollerman, J., Reinecke, M., Rpkc, F.K., Spyromilio, J. 2005, A&A, 437, 983

Kuhlen, M., Woosley, S.E., Wunsch, S. 2005, submitted to ApJ(astro-ph/0509367)

Livne, E., Asida, S.M., & Höflich, P. 2005, ApJ, 632, 443

Milne, P.A., et al. 2004, ApJ, 613, 1101

Niemeyer, J.C. 1999, ApJ, 523, L57

Plewa, T., Calder, A. C., Lamb, D. Q., 2004, ApJ, 612, L37

Reinecke, M., Hillebrandt, W., & Niemeyer, J. 2002, A&A, 391, 1167

Woosley, S.E., Wunsch, S., & Kuhlen, M. 2004, ApJ, 607, 921



Table 1. Results of the 3D simulation of the PRD model

$K$ ( $10^{51}$ erg)	M (C) ( $M_{\odot}$ )	M (O) ( $M_{\odot}$ )	M (Mg) ( $M_{\odot}$ )	M (Si) ( $M_{\odot}$ )	M ( $^{56}\text{Ni}$ ) ( $M_{\odot}$ )	$Y_e$ ( $\text{mol} \cdot \text{g}^{-1}$ )
1.05	0.06	0.15	0.05	0.28	0.70	0.4976 <sup>a</sup>

<sup>a</sup>Mean final electron mole number

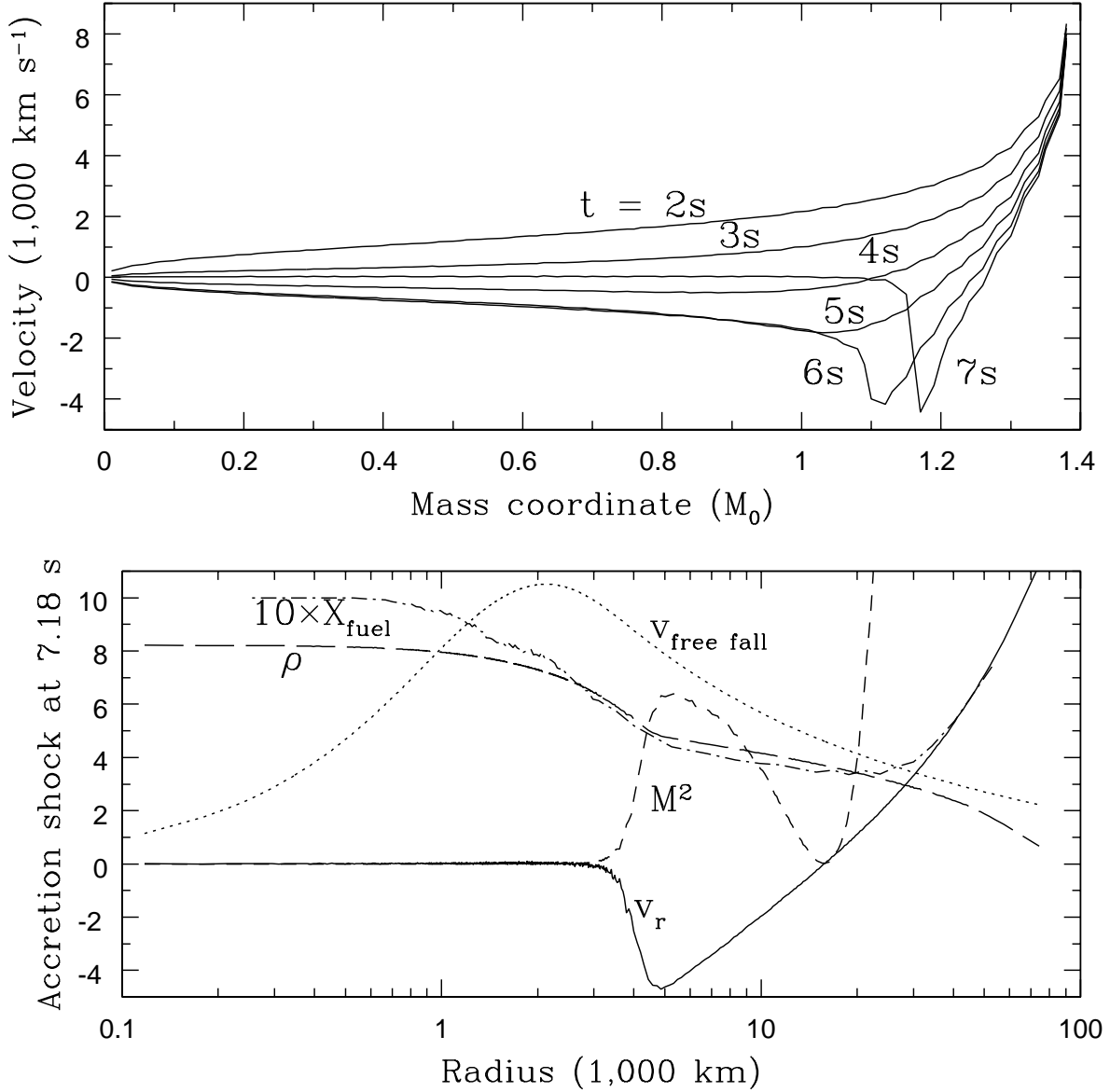


Fig. 1.— Formation of the hydrostatic core and accretion shock, whose structure is shown in the bottom panel. In the top panel there is depicted the evolution of the angle-averaged velocity profile during the pulsation of the WD, computed with a 3D hydrocode. The bottom panel shows the angle-averaged structure at the end of the pulsation, 7.18 s after thermal runaway, as a function of radius. It can be seen the hydrostatic core up to  $\sim 2,500$  km, the accretion shock at  $\sim 5,000$  km, and the expanding atmosphere above  $\sim 20,000$  km. The curves represent the angle-averaged radial velocity,  $v_r$  in units of  $1,000 \text{ km}\cdot\text{s}^{-1}$ , free fall velocity,  $v_{\text{free fall}}$  in the same units, square of the Mach number,  $M^2$ , logarithm of density,  $\rho$  in  $\text{g}\cdot\text{cm}^{-3}$ , and mass fraction of C-O,  $X_{\text{fuel}}$

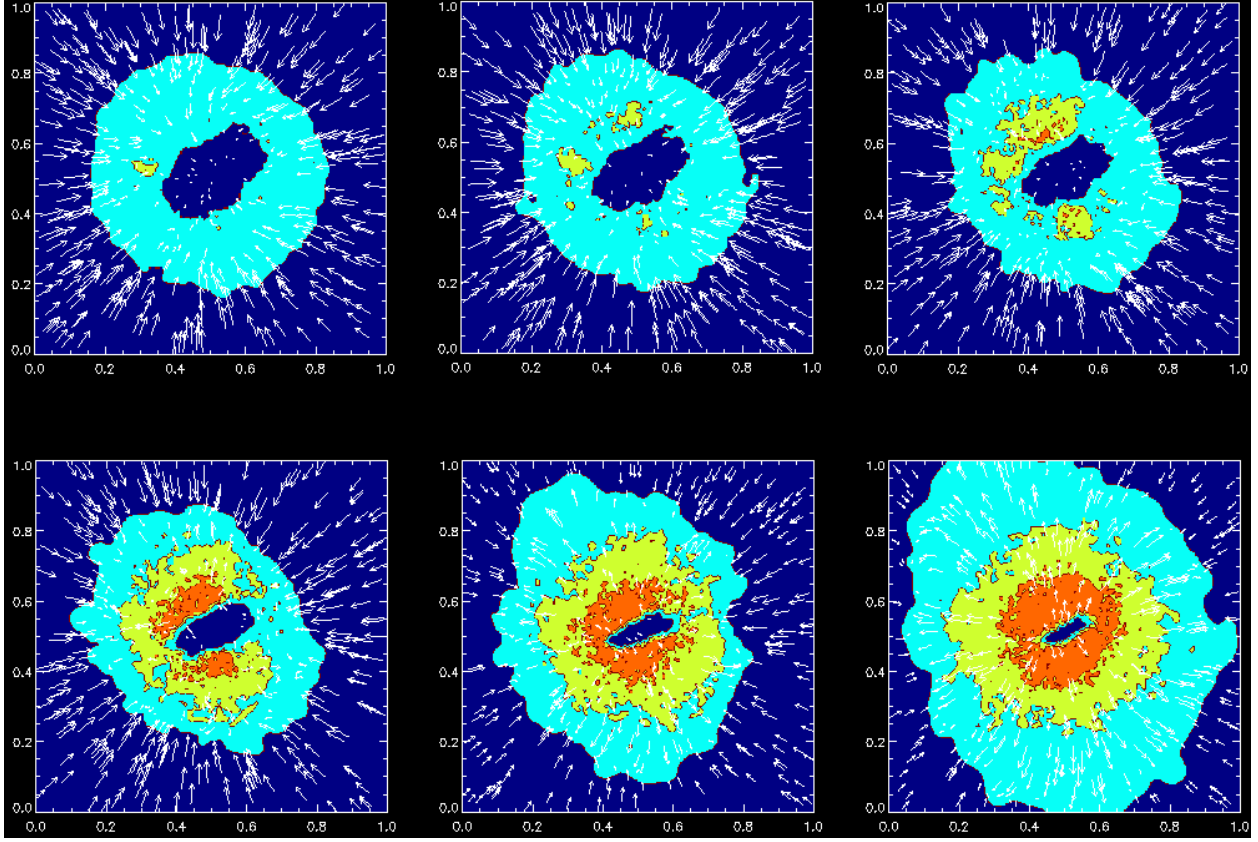


Fig. 2.— Evolution of the velocity field and isotherm contours during the detonation phase in a slice of side 10,000 km, which encloses  $\sim 85\%$  of the mass of the WD. The snapshots are shown in time steps of 0.1 s since the formation of the detonation. The temperature contours begin with  $T = 5 \times 10^8$  K and continue in steps of  $2 \times 10^9$  K. The detonation starts in several isolated hot spots (first two snapshots), afterwards propagates rapidly in azimuthal direction (third and fourth snapshots), and finally inwards in radial direction (last two snapshots). In the last snapshot it is apparent the vigorous expansion of the detonated material, which sends an inwards moving rarefaction wave that weakens the detonation front and finally quenches burning. The maximum velocities shown at each time are, from left to right and top to bottom: 6,000, 5,808, 6,844, 7,202, 10,096, and 10,986  $\text{km s}^{-1}$ . The values of the maximum resolution at each snapshot are: 20, 18, 15, 12, 11, and 11 km .[See the electronic edition of the Journal for a color version of this figure.]

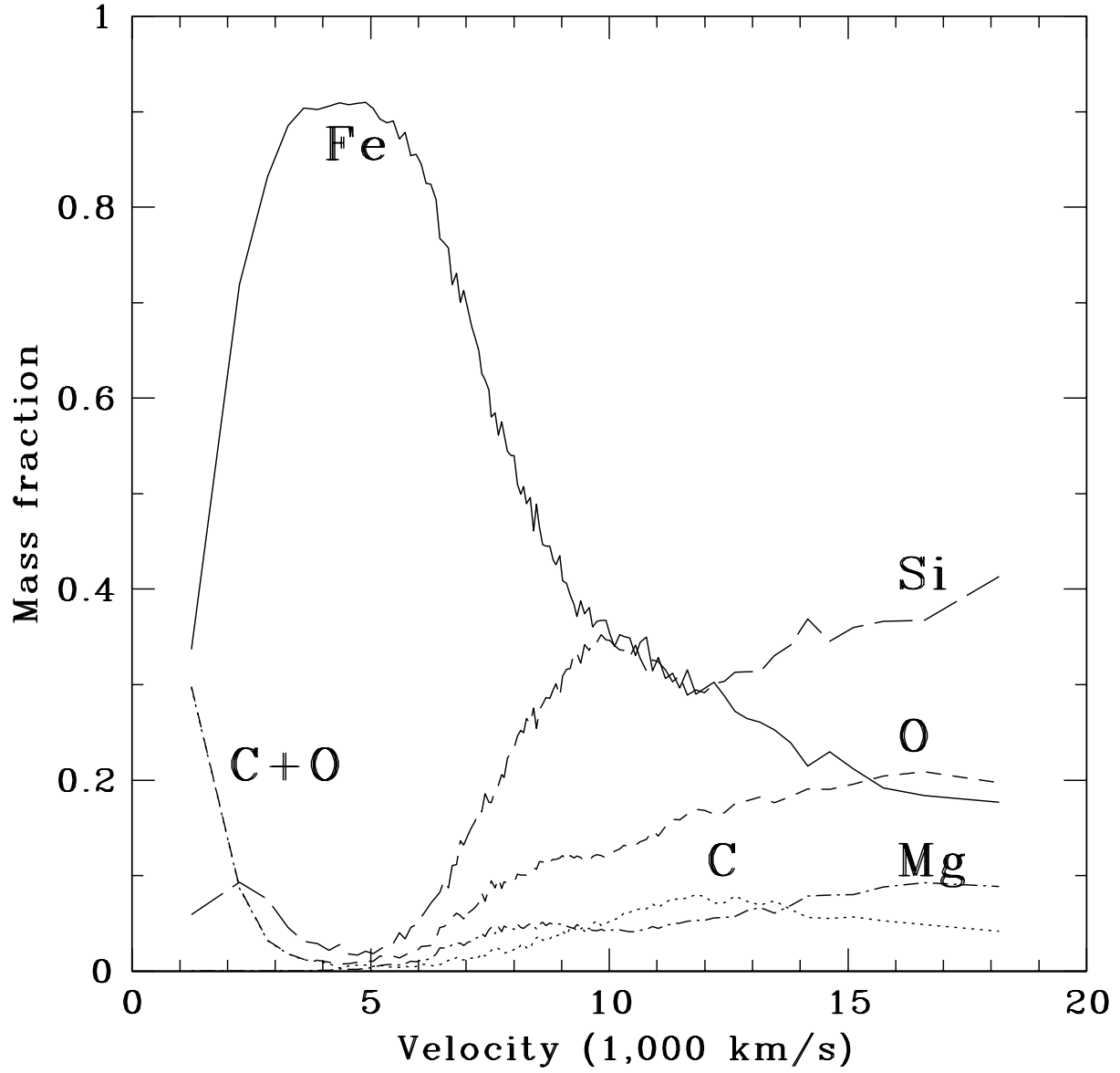


Fig. 3.— Final distribution of the main chemical elements (after radioactive decays) as a function of final velocity